



Effect of disorder on phases across two-dimensional thermal meltingPrashanti Jami ¹, Pinaki Chaudhuri,² Chandan Dasgupta,^{3,4} and Amit Ghosal ¹¹*Department of Physics, Indian Institute of Science Education and Research (IISER) Kolkata, Mohanpur 741246, West Bengal, India*²*The Institute of Mathematical Sciences, Taramani, Chennai 600113, India*³*Department of Physics, Indian Institute of Science, Bangalore 560012, India*⁴*International Centre for Theoretical Sciences, Tata Institute of Fundamental Research, Bangalore 560089, India*

(Received 31 July 2023; revised 2 April 2024; accepted 11 April 2024; published 3 June 2024)

We study melting in a two-dimensional system of classical particles with Gaussian-core interactions in disordered environments. The pure system validates the conventional two-step melting with a hexatic phase intervening between the solid and the liquid. This picture is modified in the presence of pinning impurities. A random distribution of pinning centers forces a hexaticlike low-temperature phase that transitions into a liquid at a single melting temperature T_m^{RP} . In contrast, pinning centers located at randomly chosen sites of a perfect crystal anchor a solid at low temperatures which undergoes a direct transition to the liquid at T_m^{CP} . Thus, the two-step melting is lost in either case of disorder. We discuss the characteristics of melting depending on the nature of the impurities.

DOI: [10.1103/PhysRevE.109.L062101](https://doi.org/10.1103/PhysRevE.109.L062101)

Introduction. Enhanced fluctuations make two-dimensional (2D) melting a topic of immense research interest. Unlike their three-dimensional counterparts undergoing “Lindemann melting” [1,2], 2D melting is mediated by the unbinding of topological defects. The positional order (PO) and bond-orientational order (BOO) decouple in 2D, producing a “hexatic phase” sandwiched between the solid and the liquid. Hexaticity, a rich concept, is realized in colloids [3,4], the vortex lattice in superconductors [5], active Brownian disks [6], and, recently, van der Waals magnet [7]. The celebrated Kosterlitz-Thouless-Halperin-Nelson-Young (KTHNY) theory [8–12] pictures 2D melting as a two-step process involving successive unbinding of dislocations and disclinations, presented schematically in Fig. 1(a). However, the relevance of the two-step 2D melting has also been debated [13–16].

Quenched disorder, inherent to real materials, can not only move around the phase boundaries, but is also capable of modifying the mechanism of melting. For example, impurities can generate unbounded defects even at $T = 0$, and thereby mask the unbinding of thermal defect pairs. This could strike out solidity even at the lowest T , as suggested by Nelson [17], portrayed schematically in Fig. 1(b). In contrast, impurities which pin a given fraction of particles on sites of the underlying perfect lattice could stabilize the solid by anchoring it via these commensurate locations, and thereby consume the phase space of hexaticity [see Fig. 1(c)]. The role of disorder in destabilizing the hexatic phase [18] and in enhancing long-range correlation has also been pointed out [19]. Thus, a careful analysis of 2D melting in disordered media can potentially uncover new paradigms.

Experiments on colloids [20], vortex lattices [21,22], and multicomponent mixtures [23] indicate a broadened stability of the hexatic phase in the presence of disorder that is consistent with recent calculations [24–29]. The study of 2D melting is also popular in confined geometry [30–32]

mimicking disordered background. Zeng *et al.* [33] have argued that a solid (“Bragg glass”) phase with power-law decay of translational correlations cannot occur in a 2D system with impurities. Pronounced hexatic correlations are expected to be present [34,35] if the disorder is not strong, though there are controversies [36–38] about the existence of a hexatic glass phase with long- or quasi-long-range hexatic order in 2D. The study of 2D melting on a spherical surface, in which defects are inherently embedded even at $T = 0$, has recently been carried out on a colloidal system [39].

In this Letter, we investigate the phases across melting of a bulk 2D system of soft-core particles, modeled via Gaussian-core interactions [40], which is known to validate the KTHNY melting scenario in a pure system [41]. Addressing the role of quenched disorder in the phase behavior of this model, our key results are summarized as follows: (i) Random pinning (RP) destabilizes solidity, causing a single transition from a low- T hexaticlike phase to a high- T liquid. Here, the low- T phase undergoes a likely crossover from hexatic glass to hexatic liquid. (ii) On the other hand, the commensurate pinning (CP) anchors solidity and engulfs hexaticity—even the high- T liquid phase supports inhomogeneous pockets of crystallinity. The defect locations correlate oppositely with pinning centers in the two models of disorder—defects tend to bind with the pinning centers for RP systems, whereas they stay away from the impurities in CP systems. Thus, in either realization of the quenched disorder, the two-step melting is lost.

Model and method. We introduce disorder in two different ways: (a) Random pinning (RP), in which we freeze a given fraction (n_{imp}) of particles, chosen randomly in space, within a high- T liquid configuration. Here, these immobile particles act as a disorder. (b) Commensurate pinning (CP), where the n_{imp} fraction of particles is frozen at randomly chosen positions of an ideal triangular lattice—the

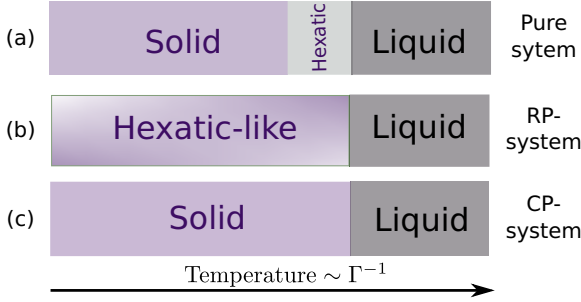


FIG. 1. A schematic representation of 2D melting in (a) KTHNY description in a pure system, (b) a system with randomly placed impurities, and (c) with a fraction of particles frozen at randomly chosen zero-temperature positions of the pure system, suggesting that the clean melting may be obscured by impurities (see text).

ground-state configuration of the pure system. Note that CP represents correlated disorder with a long-range positional correlation of a perfect lattice. In contrast, RP constitutes a nearly uncorrelated disorder, though a weak short-range correlation of a high- T liquid may exist. We investigated a system of $N = 4356$ particles, with $n_{\text{imp}} = 3.4\%$. The validity of our key findings is also established for other parameters, namely, $N = 6084$ and $n_{\text{imp}} = 2.2\%$ (see the Supplemental Material (SM) [42] for details). We focused only on weak n_{imp} in this study to elucidate the role of pinning on 2D melting. Stronger n_{imp} would cause localization of constituent particles, a phenomenon beyond our present interest. These results were compared with those from a pure system with $N = 4096$ particles. For these systems, we sample configurations via molecular dynamics (MD) [43] within the canonical ensemble, using LAMMPS [44]. We consider a simulation box having dimensions $L_x = \frac{2}{\sqrt{3}}L_y$, with periodic boundary conditions. L_x is adjusted to keep the density ρ of particles fixed for all of our studies ($\rho = 0.628$). We carried out 2×10^7 MD steps with a time step $\delta t = 0.005$. We use dimensionless parameters, $t' = t\sqrt{\epsilon/m\sigma^2}$ and $E' = E/\epsilon$, where m is the mass of each particle. T is expressed in terms of Γ^{-1} [45], where $\Gamma = \epsilon \exp(-\sqrt{3}/2\rho)/K_B T$. The physical observables are averaged over 8–10 independent pinning configurations for a given n_{imp} .

Positional and bond-orientational order. A pure 2D solid is characterized by two kinds of ordering: (i) PO measured by $\psi_T = \frac{1}{N} \langle |\Psi_T| \rangle$, where $\Psi_T = \sum_{i=1}^N \exp(i\mathbf{G} \cdot \mathbf{r}_i)$. \mathbf{G} is a first shell reciprocal-lattice vector of the underlying triangular crystal and \mathbf{r}_i is the position of particle i . (ii) BOO, quantified by $\psi_6 = \frac{1}{N} \langle |\sum_{k=1}^N \Psi_6(r_k)| \rangle$, where $\Psi_6 = \frac{1}{N_b(k)} \sum_{l=1}^{N_b(k)} \exp(i6\theta_{kl})$. The sum is over the $N_b(k)$ nearest neighbors of particle k identified by a Voronoi construction [46] and θ_{kl} is the angle that a line joining particle k and particle l makes with a reference axis. KTHNY theory predicts two critical temperatures, Γ_{SH}^{-1} and Γ_{HL}^{-1} , for the thermal depletion of quasi-long-range PO (solid to hexatic) and BOO (hexatic to liquid), respectively, leaving a hexatic phase with quasi-long-range BOO between the solid and isotropic liquid phases.

In Figs. 2(a) and 2(b), we plot the thermal evolution of ψ_T and ψ_6 for pure, RP, and CP systems. While the pure

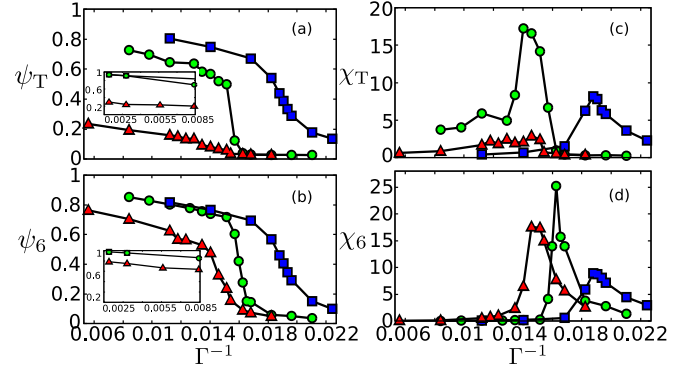


FIG. 2. Positional and orientational ordering tendencies as a function of Γ^{-1} for pure (green circles), RP (red triangles), and CP (blue square) systems. (a) Decay of PO (ψ_T) with Γ^{-1} (the inset shows ψ_T for $\Gamma^{-1} \rightarrow 0$). (b) The softening of the BOO (ψ_6). Here, $\psi_6(\Gamma^{-1} \rightarrow 0)$ is shown in the inset. (c),(d) show the corresponding susceptibilities χ_T and χ_6 . The location of the peaks in χ_T and χ_6 identify the transitions. We find $\Gamma_{\text{RP}}^{-1} = 0.0145$ from χ_6 . Interestingly, the peaks in χ_T and χ_6 for CP systems appear at the same $\Gamma_{\text{CP}}^{-1} = 0.0187$.

system follows KTHNY melting [47] with $\Gamma_{\text{SH}}^{-1} = 0.0140$ and $\Gamma_{\text{HL}}^{-1} = 0.0162$, ψ_T in the CP system is found to survive to larger T . The RP system shows a much weaker ψ_T than the other two, even at the lowest T , and depletes very gradually with T without any threshold behavior. A threshold behavior near Γ_{HL}^{-1} is also seen in the pinned systems in Fig. 2(b), albeit the transitions are broader. Unlike ψ_T , the ψ_6 is comparable at low T in pure, CP, and RP systems. We also note that ψ_T and ψ_6 show a significant drop at the same critical temperature in a CP system, implying a direct transition from solid to liquid, which we discuss further below.

In addition, the fluctuations of ψ_T and ψ_6 define generalized susceptibilities $\chi_\alpha = \frac{1}{N} [\langle |\Psi_\alpha|^2 \rangle - \langle |\Psi_\alpha| \rangle^2]$ (with $\alpha = T$ or 6) and help to identify Γ_{SH}^{-1} and Γ_{HL}^{-1} , as shown in Figs. 2(c) and 2(d). Their behavior confirms that the pure system shows sharp transitions. Consistent with our finding in Fig. 2(a), χ_T in the RP system features only a broad and low hump, hinting that a low- T phase in such a system represents a broad crossover between a hexatic glass [34] and a hexatic liquid [48]. Additional exploration of this subtle physics from the study of dynamics of 2D melting in pinned systems is in progress, and will be published elsewhere. This is, however, also consistent with the trajectory of particles in an RP system at $\Gamma^{-1} = 0.0028$, as shown in Fig. S1(d) of the SM [42]. Congruous with our findings in Figs. 2(a) and 2(b), the locations of the peak of χ_T and χ_6 verify that PO and BOO in the CP system vanish at a single Γ_{CP}^{-1} . While our results from Fig. 2 seem to support the schematic phase diagram of Fig. 1, we emphasize that the “impure” phases at low and high T defy conventional wisdom. These include the presence of unbound defects even at $T = 0$ in RP systems (consistent with Zeng *et al.* [33]), and pockets of crystallinity deep into the liquid phase in CP systems, as seen from Figs. S1(g)–S1(i) in the SM [42], and discussed below.

Defects analysis. In KTHNY theory, a 2D solid transits to the hexatic phase by the unbinding of paired dislocations

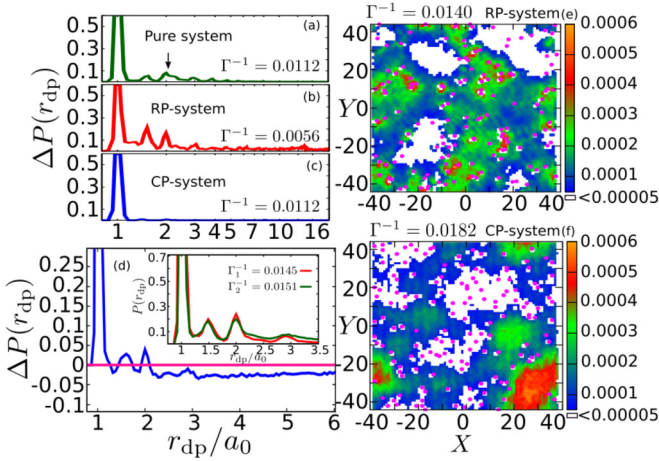


FIG. 3. The distribution of distances between dislocation pairs, $P(r_{dp})$, in different phases. (a)–(c) Results for pure, RP, and CP systems, respectively, at low T . a_0 is the average interparticle distance. $P(r_{dp})$ is sharply peaked at the typical distance between dislocation pairs, though there are differences in the details. The distribution has a short tail for the pure system, a very long tail for RP systems, and essentially no tail for CP systems. (d) $\Delta P(r_{dp})$ taken in a pure system between T 's just above and below Γ_{SH}^{-1} . The inset shows the corresponding $P(r_{dp})$. The largest zero-crossing distance of $\Delta P(r_{dp})$ is taken as r_{dp}^c , and is marked as an arrow in (a). (e), (f) The spatial density of unbound defects just prior to melting into a liquid for a given realization of the RP and CP systems. The pinning centers are marked via magenta dots.

[10,11]. We proceed to examine the consistency of this picture in Fig. 2. This requires an estimation of the critical distance between two dislocations (with equal and opposite Burger vectors) below which they are bound. We first employ the Hungarian algorithm [49], which chooses “correct” partners of dislocations by minimizing the sum of the distances between all partners [50]. The distribution of the resulting pair distances, $P(r_{dp})$, at low T is presented in Figs. 3(a)–3(c). $P(r_{dp})$ is sharply peaked for pure systems in Fig. 3(a), with insignificant weight at larger r_{dp} . In contrast, its long tail at low T [shown for $\Gamma^{-1} = 0.0056$ in Fig. 3(b)] for the RP system arises from unbound dislocations even for $T \rightarrow 0$, which destabilize a true solid. $P(r_{dp})$ in CP systems [Fig. 3(c)] consists of the initial sharp peak and nearly zero weight for larger r_{dp} . A discernible tail in $P(r_{dp})$ for pure systems develops when dislocation pairs start unbinding. An integrated distribution of $P(r_{dp})$ features a threshold behavior at this transition (see the SM [42]).

To obtain the critical r_{dp} for the pure system, we plot, in Fig. 3(d), the difference of these distributions, $\Delta P(r_{dp})$, at temperatures just above and below Γ_{SH}^{-1} , while the corresponding $P(r_{dp})$'s are shown as the inset. The total positive and negative weights of $\Delta P(r_{dp})$ cancel out, and $r_{dp}^c \approx 2.15a_0$ is identified as the last zero-crossing point. This identification is found robust for T 's near Γ_{SH}^{-1} . A study of distances of disclination pairs yielded a similar critical distance between disclination pairs. Once extracted for the pure system, these critical distances were used to analyze pinned systems. Subsequently, we explored the thermal evolution of the defects and their unbinding in Figs. 4(a)–4(c). For the

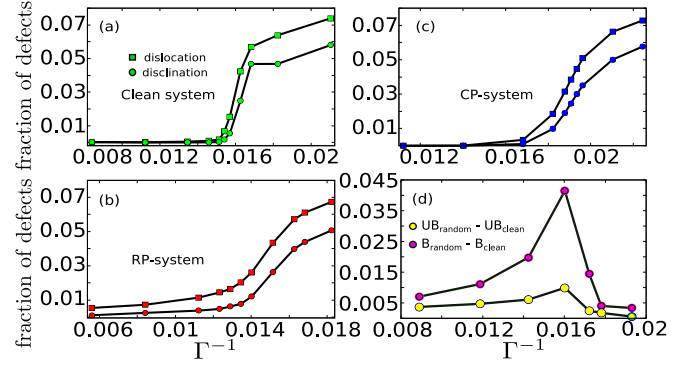


FIG. 4. Evolution of defects. (a)–(c) The variation of defects with Γ^{-1} (green: pure; red: RP; and blue: CP system). (a) The evolution of unbound dislocations (in squares) as well as disclinations (in circles) validate KTHNY melting in pure systems (traces of disclinations are multiplied by 10 for visual clarity). (b) The presence of significant dislocations in RP systems at low Γ^{-1} prohibits solidity. (c) In CP systems, the proliferation of unbound defects (both dislocations and disclinations) commences at a single threshold ($\Gamma^{-1} = 0.0198$), implying a direct solid-liquid transition. (d) The comparative number of defects in RP systems to a pure system, illustrating how the number of bound (B) and unbound (UB) defects grows with increasing temperature.

lowest T , defects are essentially absent in the pure system. Unbound disclinations proliferate at $\Gamma^{-1} \approx 0.0162$, whereas dislocations unbind at $\Gamma^{-1} \approx 0.0145$, with a hexatic phase at intervening temperatures [41], consistent with Fig. 2. The CP system [Fig. 4(c)] behaves like a “better” solid at low T due to the absence of any free defects up to $\Gamma^{-1} = 0.0182$; beyond that, unbound dislocations and disclinations start proliferating at the same Γ_{CP}^{-1} . There is a significant number of impurity-induced unbound dislocations in the RP system for $T \rightarrow 0$, as also concluded from Fig. 2. Here, unpaired dislocations are not only present for all T , they even outnumber bound dislocations at low T . Figure 4(d) addresses the role of the impurity-induced free defects (at $T \rightarrow 0$) in RP systems, on the thermal defects, whose unbinding drives the two transitions in a pure system. The number of bound (B) and unbound (UB) defects, with corresponding numbers subtracted for an equivalent pure system, are examined separately in Fig. 4(d). These numbers increase sharply with T until the system transits to the liquid. Thus, the impurity-induced defects help promote further thermal defects than in pure systems for $\Gamma^{-1} < \Gamma_{HL}^{-1}$. Such a rise disappears in the liquid. In fact, this difference in bound defects in the liquid goes down to a even lower value than the corresponding number at $T \rightarrow 0$.

Correlations. Finally, we discuss the orientational correlations as measured by the correlation function $g_6(r) = \langle \Psi_6(\mathbf{r}_i) \Psi_6^*(\mathbf{r}_j) \rangle$, where $r = |\mathbf{r}_i - \mathbf{r}_j|$. The T dependence of the orientational correlations in the pure system follows the KTHNY scenario [10–12] as claimed earlier [41]. The evolution of $g_6(r)$ for various T is shown in Fig. 5 for RP and CP systems. Our χ^2 -minimization analysis [51] of the large- r decay of $g_6(r)$ in the RP system [Fig. 5(a)] identified a power-law behavior for nearly the entire low- T phase. This power-law behavior continues until an exponential decay

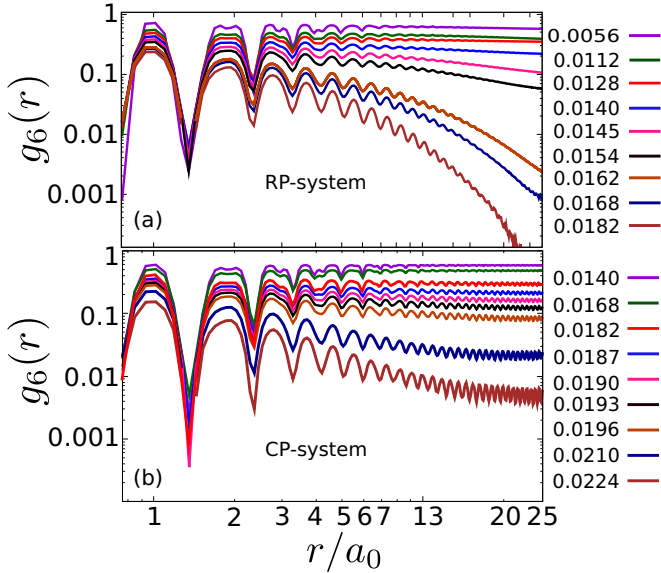


FIG. 5. Correlations. (a), (b) The orientational correlation function $g_6(r)$ of RP and CP systems, respectively, for the values of Γ^{-1} as labeled in each case. In (a), power-law decay of the correlations is visible (for $\Gamma^{-1} < \Gamma_m^{-1}$) down to a very low T in the RP system; e.g., we find $g_6(r, \Gamma^{-1} = 0.0112) \sim (r/a_0)^{-0.14}$, $g_6(r, \Gamma^{-1} = 0.014) \sim (r/a_0)^{-0.2}$, $g_6(r, \Gamma^{-1} = 0.0154) \sim (r/a_0)^{-0.64}$, while $g_6(r, \Gamma^{-1} = 0.0162) \sim \exp^{-0.16(r/a_0)}$, as shown via dashed lines. (b) In contrast, in a CP system, correlations get modified. Even in the liquid phase, the conventional exponential decay flattens out at large r , implying a “remnant crystallinity” (see text).

sets in for $\Gamma^{-1} \geq 0.0162$, signaling the onset of liquidity. Intriguingly, $g_6(r)$ in CP systems shows the enhanced solidity

for $\Gamma^{-1} \leq 0.0187$, where its traces remain largely flat. Beyond the direct melting from solid to liquid for $\Gamma^{-1} > 0.0190$, $g_6(r)$ in CP systems displays a tendency of plateauing at large r , though it decays at intermediate r . This is a signature of “remnant solidity” arising from local crystalline pockets surrounding the impurities whose locations are commensurate with the perfect crystal and hence anchoring crystallinity in the vicinity (see the SM [42]). This is a direct consequence of the correlated nature of the CP impurities.

Conclusion. To summarize, we demonstrate that the conventional picture of 2D melting undergoes significant changes in the presence of impurities. While RP disorder destabilizes solidity and CP disorder removes the hexatic phase, the low- T phase in RP systems is not the conventional hexatic. Similarly, the high- T phase in the CP systems mixes remnant solidity with the liquid phase. The inhomogeneous melting (Fig. S1 in the SM [42]) generates defects which correlate differently with pinning centers: For RP systems, the defects tend to bind with the pinning centers, whereas the defects stay away from the impurities in CP systems. While defects are found essential for driving the melting, our MD configurations indicate that they often bunch up in various shapes of macroscopic size (see the videos in the SM [42]). An extension of our study to larger systems exploring the possible role of grain boundaries on melting is a promising future direction. It will also be interesting to inspect the role of quantum fluctuations in these thermal phases. We hope that our findings will motivate future experiments to shed new light.

Acknowledgments. The authors gratefully acknowledge fruitful discussions with the late S. Sengupta at the formative stage of this study. The authors also acknowledge useful discussions with D. Dhar. A.G. acknowledges Science and Engineering Research Board (SERB) research Grant No. MTR/2022/000946 from the Government of India.

- [1] F. Lindemann, The calculation of molecular vibration frequencies, *Phys. Z* **11**, 609 (1910).
- [2] Y. E. Lozovik, Ion and electron clusters, *Sov. Phys. Usp.* **30**, 912 (1987).
- [3] K. Zahn, R. Lenke, and G. Maret, Two-stage melting of paramagnetic colloidal crystals in two dimensions, *Phys. Rev. Lett.* **82**, 2721 (1999).
- [4] U. Gasser, C. Eisenmann, G. Maret, and P. Keim, Melting of crystals in two dimensions, *ChemPhysChem* **11**, 963 (2010).
- [5] I. Guillamón, H. Suderow, A. Fernández-Pacheco, J. Sesé, R. Córdoba, J. M. De Teresa, M. R. Ibarra, and S. Vieira, Direct observation of melting in a two-dimensional superconducting vortex lattice, *Nat. Phys.* **5**, 651 (2009).
- [6] P. Digregorio, D. Levis, A. Suma, L. F. Cugliandolo, G. Gonnella, and I. Pagonabarraga, Full phase diagram of active Brownian disks: From melting to motility-induced phase separation, *Phys. Rev. Lett.* **121**, 098003 (2018).
- [7] P. Meisenheimer, H. Zhang, D. Raftrey, X. Chen, Y.-T. Shao, Y.-T. Chan, R. Yalisove, R. Chen, J. Yao, M. C. Scott, W. Wu, D. A. Muller, P. Fischer, R. J. Birgeneau, and R. Ramesh, Ordering of room-temperature magnetic skyrmions in a polar van der Waals magnet, *Nat. Commun.* **14**, 3744 (2023).
- [8] J. M. Kosterlitz and D. J. Thouless, Long range order and metastability in two dimensional solids and superfluids (Application of dislocation theory), *J. Phys. C* **5**, L124 (1972).
- [9] J. M. Kosterlitz and D. J. Thouless, Ordering, metastability and phase transitions in two-dimensional systems, *J. Phys. C* **6**, 1181 (1973).
- [10] B. I. Halperin and D. R. Nelson, Theory of two-dimensional melting, *Phys. Rev. Lett.* **41**, 121 (1978).
- [11] D. R. Nelson and B. I. Halperin, Dislocation-mediated melting in two dimensions, *Phys. Rev. B* **19**, 2457 (1979).
- [12] A. P. Young, Melting and the vector Coulomb gas in two dimensions, *Phys. Rev. B* **19**, 1855 (1979).
- [13] S. C. Kapfer and W. Krauth, Two-dimensional melting: From liquid-hexatic coexistence to continuous transitions, *Phys. Rev. Lett.* **114**, 035702 (2015).
- [14] S. T. Chui, Grain-boundary theory of melting in two dimensions, *Phys. Rev. B* **28**, 178 (1983).
- [15] W. Qi, A. P. Gantapara, and M. Dijkstra, Two-stage melting induced by dislocations and grain boundaries in monolayers of hard spheres, *Soft Matter* **10**, 5449 (2014).
- [16] M. Mazars, The melting of the classical two-dimensional Wigner crystal, *Europhys. Lett.* **110**, 26003 (2015).

- [17] D. R. Nelson, Reentrant melting in solid films with quenched random impurities, *Phys. Rev. B* **27**, 2902 (1983).
- [18] W. Qi and M. Dijkstra, Destabilization of the hexatic phase in systems of hard disks by quenched disorder due to pinning on a lattice, *Soft Matter* **11**, 2852 (2015).
- [19] I. Guillamón, R. Córdoba, J. Sesé, J. M. De Teresa, M. R. Ibarra, S. Vieira, and H. Suderow, Enhancement of long-range correlations in a 2D vortex lattice by an incommensurate 1D disorder potential, *Nat. Phys.* **10**, 851 (2014).
- [20] S. Deutschländer, T. Horn, H. Löwen, G. Maret, and P. Keim, Two-dimensional melting under quenched disorder, *Phys. Rev. Lett.* **111**, 098301 (2013).
- [21] S. C. Ganguli, H. Singh, I. Roy, V. Bagwe, D. Bala, A. Thamizhavel, and P. Raychaudhuri, Disorder-induced two-step melting of vortex matter in co-intercalated NbSe₂ single crystals, *Phys. Rev. B* **93**, 144503 (2016).
- [22] R. Duhan, S. Sengupta, R. Tomar, S. Basistha, V. Bagwe, C. Dasgupta, and P. Raychaudhuri, Structure and dynamics of a pinned vortex liquid in superconducting *a*-Re₆Zr thin film *Phys. Rev. B* **108**, L180503 (2023).
- [23] Y.-W. Li, Y. Yao, and M. P. Ciamarra, Two-dimensional melting of two- and three-component mixtures, *Phys. Rev. Lett.* **130**, 258202 (2023).
- [24] E. N. Tsiok, Y. D. Fomin, E. A. Gaiduk, and V. N. Ryzhov, Structural transition in two-dimensional hertzian spheres in the presence of random pinning, *Phys. Rev. E* **103**, 062612 (2021).
- [25] E. A. Gaiduk, Y. Fomin, E. N. Tsiok, and V. N. Ryzhov, The influence of random pinning on the melting scenario of two-dimensional soft-disk systems, *Mol. Phys.* **117**, 2910 (2019).
- [26] N. Shankaraiah, S. Sengupta, and G. I. Menon, Disorder-induced enhancement of local hexatic correlations in two-dimensional fluids, *J. Phys.: Condens. Matter* **32**, 184003 (2020).
- [27] Arjun H and P. Chaudhuri, Dense hard disk ordering: influence of bidispersity and quenched disorder, *J. Phys.: Condens. Matter* **32**, 414001 (2020).
- [28] E. N. Tsiok, D. E. Dudalov, Y. D. Fomin, and V. N. Ryzhov, Random pinning changes the melting scenario of a two-dimensional core-softened potential system, *Phys. Rev. E* **92**, 032110 (2015).
- [29] M.-C. Cha and H. A. Fertig, Disorder-induced phase transitions in two-dimensional crystals, *Phys. Rev. Lett.* **74**, 4867 (1995).
- [30] A. Melzer, A. Schella, T. Miksch, J. Schablinski, D. Block, A. Piel, H. Thomsen, H. Kählert, and M. Bonitz, Phase transitions of finite dust clusters in dusty plasmas, *Contrib. Plasma Phys.* **52**, 795 (2012).
- [31] B. Ash, J. Chakrabarti, and A. Ghosal, Static and dynamic properties of two-dimensional coulomb clusters, *Phys. Rev. E* **96**, 042105 (2017).
- [32] B. Ash, C. Dasgupta, and A. Ghosal, Analysis of vibrational normal modes for Coulomb clusters, *Phys. Rev. E* **98**, 042134 (2018).
- [33] C. Zeng, P. L. Leath, and D. S. Fisher, Absence of two-dimensional Bragg glasses, *Phys. Rev. Lett.* **82**, 1935 (1999).
- [34] E. M. Chudnovsky, Hexatic vortex glass in disordered superconductors, *Phys. Rev. B* **40**, 11355 (1989).
- [35] E. M. Chudnovsky, Orientational and positional order in flux lattices of type-II superconductors, *Phys. Rev. B* **43**, 7831 (1991).
- [36] J. Toner, Orientational order in disordered superconductors, *Phys. Rev. Lett.* **66**, 2523 (1991).
- [37] E. M. Chudnovsky, Comment on “orientational order in disordered superconductors”, *Phys. Rev. Lett.* **67**, 1809 (1991).
- [38] J. Toner, Toner replies, *Phys. Rev. Lett.* **67**, 1810 (1991).
- [39] N. Singh, A. Sood, and R. Ganapathy, Observation of two-step melting on a sphere, *Proc. Natl. Acad. Sci. USA* **119**, e2206470119 (2022).
- [40] F. H. Stillinger, Phase transitions in the Gaussian core system, *J. Chem. Phys.* **65**, 3968 (1976).
- [41] S. Prestipino, F. Saija, and P. V. Giaquinta, Hexatic phase in the two-dimensional Gaussian-core model, *Phys. Rev. Lett.* **106**, 235701 (2011).
- [42] See Supplemental Material at <http://link.aps.org/supplemental/10.1103/PhysRevE.109.L062101> for details on model and methods, snapshots of particle trajectories, insensitivity of the key findings on the system size and pinning concentration, and identification of critical distances of defects unbinding and correlations.
- [43] D. Frenkel and B. Smit, *Understanding Molecular Simulation: From Algorithms to Applications*, Vol. 1 (Elsevier, Amsterdam, 2001).
- [44] S. Plimpton, Fast parallel algorithms for short-range molecular dynamics, *J. Comput. Phys.* **117**, 1 (1995).
- [45] R. C. Gann, S. Chakravarty, and G. V. Chester, Monte Carlo simulation of the classical two-dimensional one-component plasma, *Phys. Rev. B* **20**, 326 (1979).
- [46] J. C. Tipper, FORTRAN programs to construct the planar Voronoi diagram, *Comput. Geosci.* **17**, 597 (1991).
- [47] The three phases are clearly identified by the snapshots at three representatives T 's in the SM [42], Figs. S1(a)–S1(c).
- [48] The low- T phase supports significant hexatic order ψ_6 for our model parameters, while ψ_T and the snapshots establish the amorphous and glassy nature. The Γ^{-1} dependence of ψ_6 and ψ_T is indicative of a crossover from a hexatic glass to a hexatic liquid, before the RP system transits to a liquid at Γ_{RP}^{-1} . However, the resolution of our simulation is inadequate for drawing a firm conclusion.
- [49] H. W. Kuhn, The Hungarian method for the assignment problem, *Naval Res. Logist. Qtrly.* **2**, 83 (1955).
- [50] M. H. Lau and C. Dasgupta, Numerical investigation of the role of topological defects in the three-dimensional Heisenberg transition, *Phys. Rev. B* **39**, 7212 (1989).
- [51] K. Levenberg, A method for the solution of certain non-linear problems in least squares, *Q. Appl. Math.* **2**, 164 (1944).